Neurotherapeutics (2014) 11:623–635
DOI 10.1007/s13311-014-0269-y

ORIGINAL ARTICLE

Lentiviral-Induced High-Grade Gliomas in Rats: The Effects of *PDGFB*, *HRAS-G12V*, *AKT*, and *IDH1-R132H*

John Lynes · Mia Wibowo · Carl Koschmann · Gregory J. Baker · Vandana Saxena · A. K. M. G. Muhammad · Niyati Bondale · Julia Klein · Hikmat Assi · Andrew P. Lieberman · Maria G. Castro · Pedro R. Lowenstein

Published online: 22 April 2014

Abstract In human gliomas, the RTK/RAS/PI(3)K signaling pathway is nearly always altered. We present a model of experimental gliomagenesis that elucidates the contributions of genes involved in this pathway (*PDGF-B ligand*, *HRAS-G12V*, and *AKT*). We also examine the effect on gliomagenesis by the potential modifier gene, *IDH1-R132H*. Injections of lentiviral-encoded oncogenes induce *de novo* gliomas of varying penetrance, tumor progression, and histological grade depending on the specific oncogenes used. Our model mimics hallmark histological structures of high-grade glioma, such as pseudopalisades, glomeruloid microvascular proliferation, and diffuse tumor invasion. We use our model of gliomagenesis to test the efficacy of an experimental brain tumor gene therapy. Our model allowed us to test the contributions of oncogenes in the RTK/RAS/PI(3)K pathway, and their potential modification by over-expression of mutated IDH1, in glioma development and progression in rats. Our model constitutes a clinically relevant system to study gliomagenesis, the effects of modifier genes, and the efficacy of experimental therapeutics.

Key Words Gene therapy · HSV1-TK · adenoviral vectors · brain tumors

Introduction

Glioblastoma multiforme (GBM) is the most common primary brain tumor in adults, the incidence of which peaks between 45 and 75 years of age [1]. Despite recent advances in surgery and tumor-targeted radio- and chemotherapy, patients continue to succumb to this devastating disease within 18–21 months of initial diagnosis [2]. Novel therapies are desperately needed to extend significantly the overall survival of patients diagnosed with malignant glioma.

Traditional experimental rat glioma models utilize tumor cell lines established through the introduction of chemical carcinogens [3–6]. Despite our reliance on these models over the last several decades, it is generally thought that brain tumors created in this way may not faithfully represent human gliomagenesis, as human brain tumor formation is thought to depend on specific genomic alterations. Models of gliomagenesis initiated by the introduction of gene-specific alterations through transgenic animals or viruses have been proposed as more representative model systems. These endogenous glioma models have been successful owing to the fact that these tumors display genetic heterogeneities and resemble human gliomas [7, 8].

Whole-genome sequencing of human tumors has shown that high-grade gliomas are characterized by genetic alterations in three main pathways: i) the receptor tyrosine kinase (RTK)/rat sarcoma viral oncogene homolog (*RAS*)/phosphatidylinositol 3'-kinase (*PI3K*) signaling axis, which is associated with increased cell proliferation/protein translation;

Electronic supplementary material The online version of this article (doi:10.1007/s13311-014-0269-y) contains supplementary material, which is available to authorized users.

J. Lynes · M. Wibowo · C. Koschmann · G. J. Baker · V. Saxena · A. K. M. G. Muhammad · N. Bondale · J. Klein · H. Assi · M. G. Castro · P. R. Lowenstein (✉)
Department of Neurosurgery, University of Michigan, School of Medicine, 4570 MSRB II, 1150 West Medical Center Drive, Ann Arbor, MI 48109, USA
e-mail: pedrol@umich.edu

J. Lynes · M. Wibowo · C. Koschmann · G. J. Baker · V. Saxena · A. K. M. G. Muhammad · N. Bondale · J. Klein · H. Assi · M. G. Castro · P. R. Lowenstein
Department of Cell and Developmental Biology, University of Michigan, School of Medicine, Ann Arbor, MI 48109, USA

A. P. Lieberman
Department of Pathology, University of Michigan, School of Medicine, Ann Arbor, MI 48109, USA

ii) the *p14ARF*/*CDKN2A* and *TP53* signaling pathway, which is associated with loss of apoptotic control; and iii) the *RB*/*INK4a* signaling pathway, which is associated with cell cycle progression [9, 10]. In adult human gliomas, RTK/RAS/PI3K signaling is altered in 88 % of tumors [11]. While many animal models have manipulated this pathway, the contributions of the individual oncogenes (*PDGF-B ligand*, *HRAS-G12V*, and *AKT*) have not been elucidated. Additionally, as the majority of low-grade gliomas and secondary glioblastomas carry a mutation in *IDH1* (R132H) [12–14], we wished to determine the contribution of this mutation to gliomagenesis.

Genetically engineered animal models of high-grade gliomas are helpful in understanding the role of genes mutated in human tumors, and provide a relevant platform upon which to screen new therapies. Transgenic rodents can be created with germline deletions in tumor suppressor genes or with the addition of oncogenes, either globally or in specific cell types. A challenge for these models is that induced mutations are expressed in all cells and tissues from early stages of development. However, human glioma formation is likely to be a stochastic event with mutations occurring in single cells, resulting in clonal expansion [15].

To mimic human tumors, various systems have been developed to introduce somatic mutations into a restricted number of cells. For example, the Sleeping Beauty Transposon system has been used to stably incorporate oncogenes encoded on nonviral plasmids into the brains of newborn mice [16]. Other systems previously used to create endogenous gliomas include the RCAS/tv-a system in mice [17], retroviral vectors in rats and mice [18], and lentiviral vectors in mice [19]. Lentiviruses are ideally suited for the establishment of *de novo* gliomas owing to their ability to transduce both dividing and nondividing cells, and encoding large transgenic (>10 kb) DNA sequences, and have not been previously reported in rat models of glioma.

In this study, we achieved endogenous gliomas of varying penetrance, tumor progression, and histological grade using lentiviral vectors in adult rats, and elucidated the contributions of individual oncogenes and modifier genes in an animal model of human glioma.

Methods

Lentivirus and Adenovirus Production

We used fourth-generation, self-inactivating, replication-deficient, VSV-G pseudotyped lentiviral vectors to induce gliomagenesis. The complementary DNA (cDNA) for human platelet-derived growth factor (PDGF)-β (*PDGFB*) was a kind gift from Dr. Eric Holland (Memorial Sloan-Kettering Cancer Center), while the cDNAs for constitutively active *AKT* and *HRAS-G12V* were kindly donated by Dr. Inder Verma (The Salk Institute for Biological Studies). Human *IDH1* cDNA was purchased from Open Biosystems (Huntsville, AL, USA) with the *IDH1-R132H* point mutation being introduced using Stratagene's QuikChange II Site-directed Mutagenesis Kit (Stratagene, La Jolla, CA, USA). cDNAs were subcloned into the lentiviral vector plasmids pLVX–Puro (Clontech, Mountain View, CA, USA) and pLVX–Puro–IRES–mCitrine to make the plasmids pLVX–Puro–*PDGFB*, pLVX–Puro–*AKT*, pLVX–Puro–*HRAS–G12V*, pLVX–Puro–*IDH1*–IRES–mCitrine, and pLVX–Puro–*IDH1–R132H*–IRES–mCitrine, all under the control of the major immediate early human cytomegalovirus promoter (see Supplementary Fig. 1 for gene construct details). Lentiviral vectors were rescued by cotransfection with Packing Mix (Clontech) into 293-TX cells (Clontech), according to the manufacturer's instructions. After 3 days, cell culture supernatant containing lentiviral particles was collected and concentrated by ultracentrifugation. Infectious lentiviral titers were determined by end-point dilution on HT1080 cells (Clontech) followed by puromycin selection. One week later, cresyl violet staining was used to quantify puromycin-resistant colonies to determine the lentiviral titer. All viral preparations exhibited undetectable levels of replication-competent lentivirus and lipopolysaccharide contamination. Treatment of high-grade gliomas was performed using first-generation adenovirus (serotype-5) expressing herpes simplex virus type 1-thymidine kinase (Ad-TK). The adenovirus was generated using a previously described method [20].

Animal Studies

Seven-to-10-week-old adult Sprague Dawley rats (Harlan, Indianapolis, IN, USA) weighing 180–220 g were used in the experiments. All animal studies were conducted according to the guidelines approved by the University Committee on Use and Care of Animals at the University of Michigan. Endogenous gliomas were generated by intracranial injections of various combinations of lentivirus expressing *PDGFB*, *HRAS-G12V*, and/or *AKT* at a volume of 1 μl per lentiviral vector delivered in a total volume of 3 μl using 0.9 % saline as a carrier solution. For survival studies, animals were monitored daily for signs of morbidity, including ataxia, impaired mobility, hunched posture, seizures, and nasal/periorbital hemorrhage. Animals displaying symptoms of morbidity were perfused by intracardial perfusion of Tyrode's solution, followed with fixation using 4 % paraformaldehyde in phosphate buffered saline. Rat brains were then removed from the skull and processed for histology. Tumor progression was assessed by sacrificing rats and determining tumor size on days 7, 14, 21, and 28 post-lentiviral injection.

PDGF-β protein secretion was confirmed by enzyme-linked immunosorbent assay, while Flag-tagged HRAS–G12V and HA-tagged AKT protein expression were

confirmed using immunohistochemistry against their respective tags. IDH1 and IDH1–R132H protein expression was confirmed via Western blot and immunohistochemistry using anti-IDH1 primary antibodies or primary antibodies specifically recognizing the sequence of amino acids involving the IDH1–R132H point mutation, a kind gift from Dr Von Deimling (German Cancer Research Center) (see Supplementary Table 1 for antibody details) [21].

Animals receiving gene therapy were given intracranial injections of 3 μl of Ad-TK (or normal saline as a control) on day 14 or 23 post-lentivirus injection using the same coordinates and burr hole used to establish the tumor. Beginning 24 h post-Ad-TK treatment, animals were administered, intraperitoneally with ganciclovir (Roche, San Francisco, CA, USA) at a dose of 25 μg/kg twice daily for 1 or 3 cycles on 10 consecutive days.

In vivo Stereotactic Lentiviral Vector Injection

We have previously described a detailed methodology for stereotactic gene transfer into the rat brain [22]. Briefly, following anesthesia, rat's crania were secured using a stereotactic frame. A midline incision was then made over the cranium and a burr hole was made 2.0 mm lateral and 2.5 mm rostral relative to the bregma. A total volume of 3 μl lentiviral particles was then delivered at 3 depths from the surface of the brain (3.0, 3.5, and 4.0 mm ventral), with 1 μl of the total volume of 3 μl being delivered at each depth. All lentiviral injections were made at a flow rate of 0.2 μl per min. The same coordinates and total volume were used when delivering adenoviral particles for gene therapy.

Cell Culture and Transfection

293 T cells were cultured in Dulbecco's modified Eagle's medium (Gibco, Carlsbad, CA, USA) with 10 % heat-inactivated fetal bovine serum, 0.3 mg/ml L-glutamine, and 50 U/ml penicillin and 50 μg/ml streptomycin. For expression of wildtype and mutant *IDH1*, 293 T cells were transfected with either pLVX–Puro–*IDH1*–IRES–mCitrine or pLVX–Puro–*IDH1–R132H*–IRES–mCitrine, respectively, using the JetPrime (Polyplus-transfection Inc., New York, NY, USA) transfection reagent according to manufacturer's instructions, with the exception that transfection mix was added to cells in suspension prior to plating.

Immunohistochemistry and Cresyl Violet (Nissl) Staining

Rat brains were fixed in 4 % paraformaldehyde for an additional 48 h at 4 °C prior to sectioning using a vibratome set to 60 μm in the z-direction. Both cresyl violet and immune-based staining of brain tissue sections were performed using previously described standard protocols (see Supplementary Table 1 for a full list of antibodies and their dilutions) [22].

Microscopic Analysis

Images were obtained using brightfield/epifluorescence (Zeiss Axioplan 2; Carl Zeiss MicroImaging, Jena, Germany), or laser scanning confocal microscopy (Leica DMIRE2; Leica Microsystems, Buffalo Grove, IL, USA) and analyzed using LSM5 software (Carl Zeiss MicroImaging). Tumor volume and stereological quantification of $Ki67^+$ cells were done using StereoInvestigator software (Microbrightfield, Williston, VT, USA). To measure tumor volume, every ninth serial brain section was selected. Throughout the enter rat brain. These sections were then stained with cresyl violet to visualize gross micoanatomical features. The tumor mass was measured using point counting at low magnification (1.25× objective), and the volume was determined using the Cavalieri estimator at a grid size of 100 μm. To quantify the number of proliferating cells, 3 sections representing the anterior, middle, and posterior aspects of the tumor were randomly selected and immunolabeled for Ki67. The tumor border was initially delineated using low magnification, followed by quantification of $Ki67^+$ cells in 10 random 150-μm square grids using high magnification (40× objective). Data were reported as the average number of $Ki67^+$ cells per 10 high magnification fields of view.

Statistical Analysis

Kaplan–Meier survival curves were statistically analyzed using the Mantel–Cox log-rank method as performed by GraphPad Prism software (GraphPad, San Diego, CA, USA). Differences in tumor volume were statistically analyzed using one-way analysis of variance followed by Tukey's post-tests using NCSS statistical and power analysis software (NCSS, East Kaysville, UT, USA). Differences were considered significant at the $p<0.05$ level.

Results

The Combination of *HRAS-G12V* and *PDGFB* Creates *De Novo* Gliomas with Rapid Tumor Progression, Full Penetrance, and High-grade Histology

We used various combinations of lentiviral vectors encoding proto-oncogenes (i.e., *PDGFB* and *IDH1*); constitutively active oncogeneic mutants (*HRAS–G12V*, *AKT*); and an overexpressed modifier gene (*IDH1-R132H*) (Supplementary Fig. 1) to assess their ability to induce *de novo* gliomas. Tumor-related morbidity was variable and depended on the specific combination of lentiviral vectors used (Fig. 1, Table 1). Animals injected with combinations of lentivirus containing *HRAS–G12V* and *PDGFB* achieved fully penetrant tumors of high-grade histology and rapid tumor progression. Gliomas

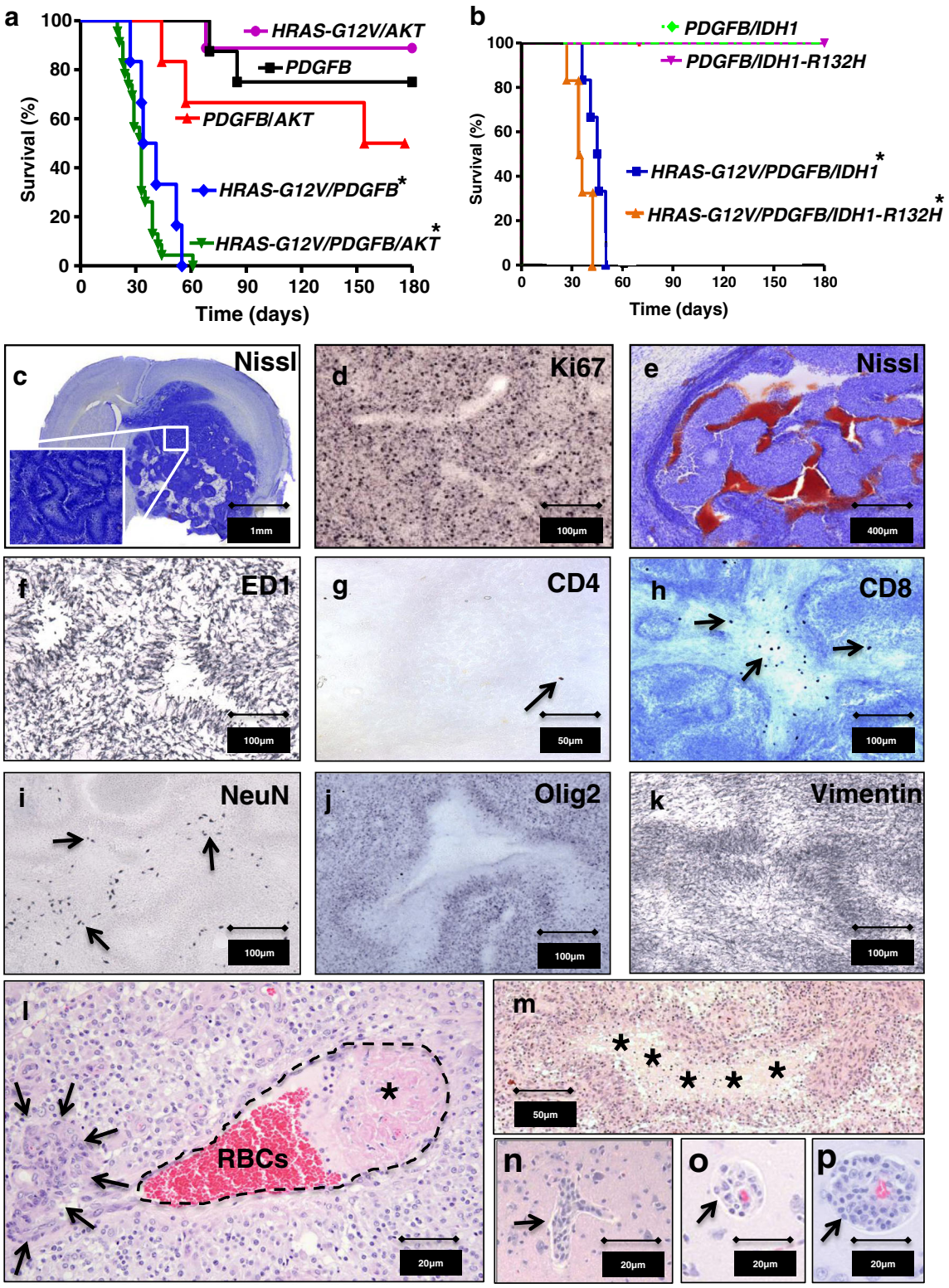

induced with the combination of *HRAS–G12V/PDGFB/AKT* displayed all the hallmarks of human GBM, including necrotic regions surrounded by pseudopalisading tumor cells, glomeruloid microvasculature proliferation, high proliferation index, and diffuse tumor invasion (Fig. 1C–P).

Analysis of high-grade gliomas induced by the combination of (*HRAS–G12V/PDGFB/AKT*) indicated that lentiviral vectors were capable of infecting a wide-range of cell-types, including astrocytes, oligodendrocytes, endothelial cells, and microglia (Supplementary Fig. 2). As the majority of tumor

◀ **Fig. 1** Specific oncogene combinations determine tumor progression, penetrance, histological grade, and lethality of lentivirus-induced gliomas. (A) Kaplan–Meier survival analysis of Sprague Dawley rats injected with various combinations of lentivirally-encoded oncogenes. *HRAS–G12V/PDGFB* and *HRAS–G12V/PDGFB/AKT* induced fully penetrant tumors within 60 days of lentiviral injection (*$p<0.001$ *vs HRAS–G12V/AKT*; *PDGFB*; and *PDGFB/AKT*). Tumors induced by *HRAS–G12V/AKT*, *PDGFB*, and *PDGFB/AKT* each had longer latencies, and varying penetrance. See Table 1 for details. (B) Effect of *IDH1–R132H* on gliomagenesis. The *IDH1–R132H* point mutation did not significantly alter tumor progression, penetrance, or lethality of tumors compared with lentiviral combinations using wildtype *IDH1*. *$p<0.001$ *vs PDGFB/IDH1* and *PDGFB/IDH1–R132H*. (C–P) Tumors induced with *HRAS–G12V/PDGFB* display histological characteristics of human high-grade gliomas. Representative coronal brain tissue section bearing a late-stage, high-grade, glioma induced by *HRAS–G12V, PDGFB*, and *AKT* (C). Nissl stain (blue) strongly labels glioma cells and outlines the tumor border. High magnification of the area outlined by the white box reveals the presence of pseudopalisading glioma cells not apparent at lower magnification. (D) High-grade *de novo* gliomas display a high cell proliferation index as indicated by the large number of Ki67-positive cells within the tumor center and (E) exhibit several areas of tumor necrosis. Large numbers of ED1-positive microglia (F) can been seen within tumor masses, with only moderate effector lymphocyte infiltration, as indicated by low numbers of $CD4^+$ (arrow in G) and $CD8^+$ (arrows in H) T-cells. NeuN-positive neuronal nuclei can be seen between pseudopalisade structures (arrows in I), indicative of the presence of normal tissue within the growing tumor mass. The majority of tumor cells in these high-grade tumors were (J) Olig2- or (K)Vimentin-positive, demonstrating a predominance of oligodendroglial and astroglial precursor cell populations, respectively. Other histological features in common with human high-grade glioma include glomeruloid vascular proliferation (arrows in L), and thrombosis (asterisk in L). The area in L encompassed by the dotted black line outlines a tumor blood vessel containing red blood cells (RBCs). Pseudopalisades are found with a characteristic necrotic core (asterisks in M). Infiltrative tumor cells are found concentrically accumulating around normal brain microvessels (arrows in N–P). See Supplementary Fig. 3 for larger sized images of (L–P)

cells in these high-grade tumors were Nestin-, Olig2-, and Vimentin-positive, it suggests that these tumors were derived from oligodendrocyte and/or astrocyte precursor populations; nevertheless, definite classification of the lineage leading to these high grade gliomas will require further detailed lineage tracing studies.

PDGFB Hastens Tumor Progression of *HRAS–G12V*-induced Gliomas

Animals injected with combinations of lentivirus containing *HRAS–G12V*, in the absence of *PDGFB* (i.e., *HRAS–G12V* alone; *HRAS–G12V/AKT*; *HRASG12V/IDH–R132H*; *HRAS–G12V/AKT/IDHR–132H*) achieved gliomas in ~75 % of rats, except for the combination of *HRASG12V/AKT* (Fig. 1A, B), suggesting that *HRAS–G12V* alone is sufficient for *de novo* tumor formation. However, in the absence of *PDGFB* gene expression, the time to tumor progression was substantially extended by approximately 6 months. Gliomas derived from lentivirus encoding *HRAS–G12V* (with or without *AKT*) showed variability in histological grade, exhibiting both low- and high-grade tumors (Table 1A).

Low-grade gliomas resulting from injection of *HRAS–G12V/AKT* were characterized by nuclear atypia, low levels of mitosis, and moderate endothelial proliferation, but lacked the hallmark features of high-grade tumors (Table 1B). These tumors also exhibited the predilection of $Vimentin^+$ and $Nestin^+$ cells to localize around neurovasculature both within the tumor center and at the periphery, where tumor cells infiltrated the normal brain (Fig. 2).

PDGFB expression hastened the progression of glioma formation, as each lentiviral combination with *HRAS–G12V* in the absence of *PDGFB* created tumors that were less penetrant than those expressing *PDGFB*. However, despite this fact, *HRAS-G12V*-derived gliomas did show the hallmark signs of high-grade pathology, including pseudopalisading cells, glomeruloid microvasculature, and vasculature-associated thrombus.

IHD1-R132H does not Alter *De Novo* Glioma Induction or Progression

We found no significant difference between animals injected with *IDH1* or *IDH1–R132H* in terms of tumor penetrance or tumor progression (Fig. 1B, Supplementary Table 2). In the absence of clinical signs we examined brains of non-symptomatic animals at 6 months infected with PDGFB/IDH1–R132H (n=6) and AKT/IDH1–R132H (n=4), and found no evidence of small- or lower-grade glial tumors. We validated *IDH1–R132H* vector expression *in vitro* using Western blot, and *in situ* using immunohistochemisty. Both methods confirmed the hypermethylated phenotype given by the *IDH1–R132H* point mutation (Supplementary Fig. 1D, E).

A Detailed Investigation of Pseudopalisade Formation and Tumor Infiltration in High-grade *De Novo* Gliomas

The near ubiquitous presence of pseudopalisades within gliomas induced with the combination of *HRAS–G12V/PDGFB/AKT* allowed for a detailed investigation of their cytology, growth, and interaction with surrounding normal brain tissue (Fig. 3). Pseudopalisade centers found within these tumors were predominantly necrotic with few remaining cells expressing HRAS–G12V and AKT protein, Nestin, and Vimentin (Supplementary Fig. 1B). Nestin-positive/Vimentin-positive (i.e., tumor) cells also constituted the majority of cells in the high-density ring of each pseudopalisade (Fig. 3A–C). Glial fibrillary acidic protein- and myelin basic protein-positive cells were invariably found outside palisading tumor cells, neuronal nuclei (NeuN)-positive neurons were also distant from these structures (Fig. 3D, E).

We sought to demonstrate the degree of infiltration in *HRAS–G12V/PDGFB/AKT* gliomas using Vimentin, an

Table 1 Summary of the tumor progression, penetrance, and neuropathology of *de novo* gliomas. (A) Tumors resulting from combinations of lentiviral vectors encoding *HRAS–G12V* and *PDGFB* exhibit full penetrance, rapid tumor progression, and high-grade histology, while tumors resulting from lentiviral vectors encoding *HRAS–G12V,* in the absence of *PDGFB*, are of mixed grade, show high penetrance, but have slower tumor progression (approximately 6 months from the time of lentivirus injection). Tumors resulting from lentiviral vectors encoding *PDGFB*, in the absence of *HRAS-G12V* have low penetrance, with slow tumor progression, yet are of high-grade histology. (B) Patterns of histology seen in the tumor models from (A). The most aggressive histology is seen when *HRAS–G12V* and *PDGFB* are combined (first column in red). These high-grade gliomas form pseudopalisades with high frequency. *HRAS–G12V* models, without *PDGFB*, develop with high frequency, but less malignant behavior, either with (high-grade, green column) or without (low-grade, blue column) necrosis/pseudopalisades. Interestingly, thrombus formation was only seen in high-grade *HRAS-G12V* in the absence of *PDGFB*

a

Lentivirus Combination	# Rats with Tumor	Tumor Progression	Grade
Rapid Growth/High Penetrance:			
HRAS-G12V/PDGFB	6/6	Rapid (<60 days)	High
HRAS-G12V/PDGFB/AKT	33/33	Rapid (<60 days)	High
HRAS-G12V/PDGFB/IDH1	6/6	Rapid (<60 days)	High
HRAS-G12V/PDGFB/IDH1-R132H	6/6	Rapid (<60 days)	High
Slow Growth/High Penetrance:			
HRAS-G12V	3/4	Slow (>60 days)	Low/High
HRAS-G12V/AKT	11/12	Slow (>60 days)	Low/High
HRAS-G12V/IDH-R132H	3/4	Slow (>60 days)	Low/High
HRAS-G12V/AKT/IDH-R132H	3/4	Slow (>60 days)	Low/High
Slow Growth/Low Penetrance:			
PDGFB	4/14	Slow (>60 days)	High
PDGFB/AKT	3/6	Slow (>60 days)	High
PDGFB/IDH1	0/6	--	--
PDGFB/IDH1-R132H	0/6	--	--
Other:			
AKT	0/4	--	--
AKT/IDH-R132H	0/4	--	--

b

Glioblastoma Feature:	HRAS-G12V+ PDGFB (High-grade)	HRAS-G12V (High-grade)	HRAS-G12V (Low-grade)
Nuclear Atypia	++	++	+
Mitosis	++++	+	+
Endothelial Proliferation	+++	++	+
Glomeruloid Structures	-	++	-
Necrosis	+	+	-
Pseudopalisades	++++	+	-
Vascular Fibrin Thrombi	-	+	-

intermediate filament protein overexpressed in malignant gliomas, as a surrogate marker for tumor cells, Tuj-1 as a marker for neuronal axons, and NeuN as a marker of neuronal nuclei. We found areas of normal brain as large as one-third of the tumor mass infiltrated by diffuse tumor cells (Fig. 4). Tuj1 and NeuN immunolabeled brain tissue sections revealed bundles of neuronal axons trapped between tumor cells in the central areas of the tumor mass (Fig. 4D, E), suggesting the existence of a larger area of tissue invasion.

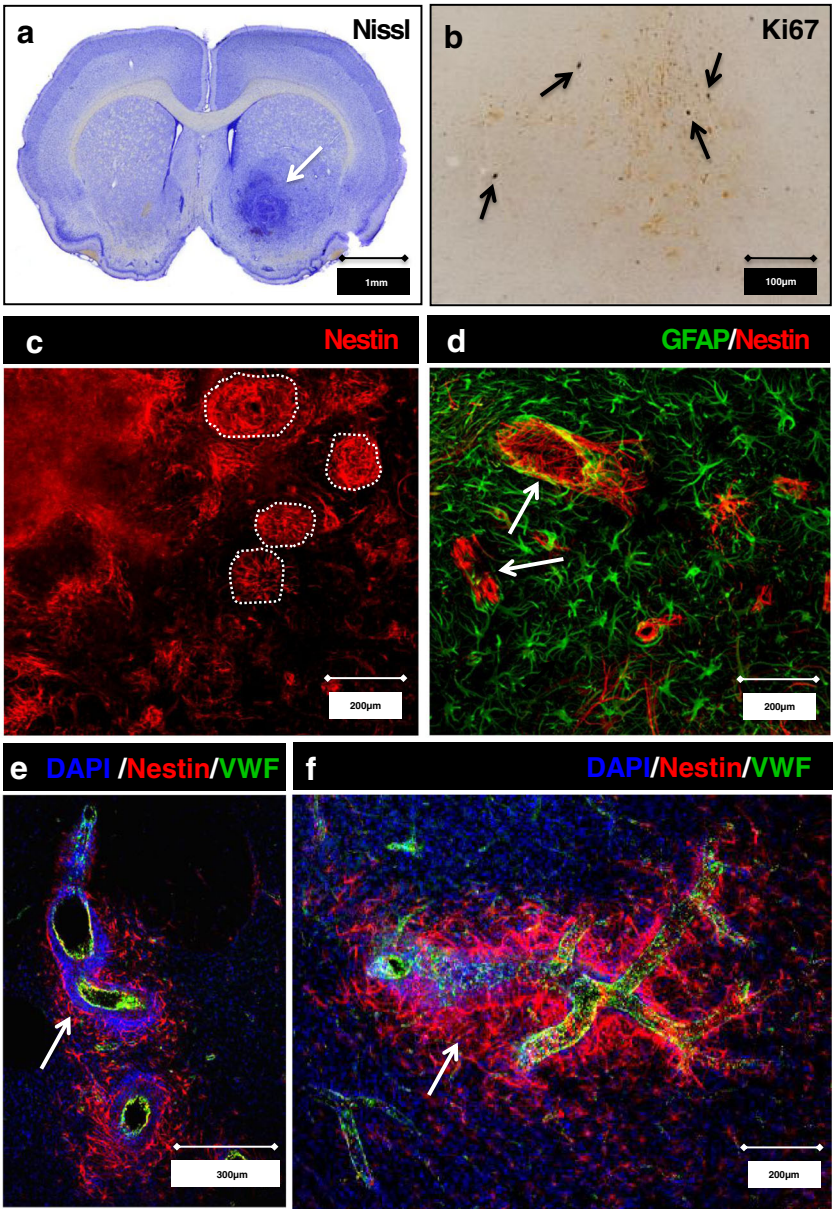

Fig. 2 Low-grade gliomas result from the combination of *HRAS–G12V* and *AKT*. (A) Representative low-grade glioma induced by *HRAS–G12V*/*AKT* and stained with Nissl to visualize gross tumor morphology. Arrow points to a significantly smaller sized tumor than seen in (Fig. 1C) induced by *HRAS–G12V*/*PDGFB*. (B–F) Low-grade gliomas were characterized by a low proliferation index as assessed by Ki67 immunolabeling (arrows in B). Patchwork rosettes of Nestin-positive tumor cells can be seen (dotted white outlines in C). Nestin-positive tumor cells exhibited a predilection for brain neurovasculature, as seen by Nestin-positive tumor cells assuming vessel morphology as they push away glial fibrillary acidic protein (GFAP)-positive astrocytes to gain access to blood vessels in (D). Nestin-positive tumor cells could also be seen in direct association with Von Willebrand factor (VWF)-positive neurovasculature (E, F). Nuclei have been labeled with 4',6-diamidino-2-phenylindole (blue)

The Response to Adenoviral-mediated Gene Therapy in High-grade *De Novo* Glioma is Dependent on the Extent of Tumor Burden

Taking advantage of the complete penetrance and the rapid and predictable tumor development of the *HRAS–G12V*/*PDGFB*/*AKT*-induced high-grade gliomas, we performed a time course analysis of high-grade tumor progression. We investigated histology and tumor volumes at 7-, 14-, 21-, and 28- days post-lentiviral injection to track tumor progression and pathology (Fig. 5). The greatest increase in tumor growth occurred between days 21 and 28 post-lentiviral injection, at which point all of the features of stage IV GBM were present (Fig. 5A, B).

We treated these high-grade gliomas either at early time points in their development, before pseudopalisade formation, or late in their development, after the formation of these structures, with Ad-TK adenoviral-mediated, conditionally cytotoxic, gene therapy. Rat survival rate significantly improved when treated at day 14 post-lentiviral injection (Fig. 5C). However, survival rates were similar to controls when rats were treated at day 23 post-injection, corresponding to larger tumor burden (Fig. 5D).

Discussion

Using lentiviral vectors stereotactically injected into the striata of adult Sprague Dawley rats, we elucidated the individual

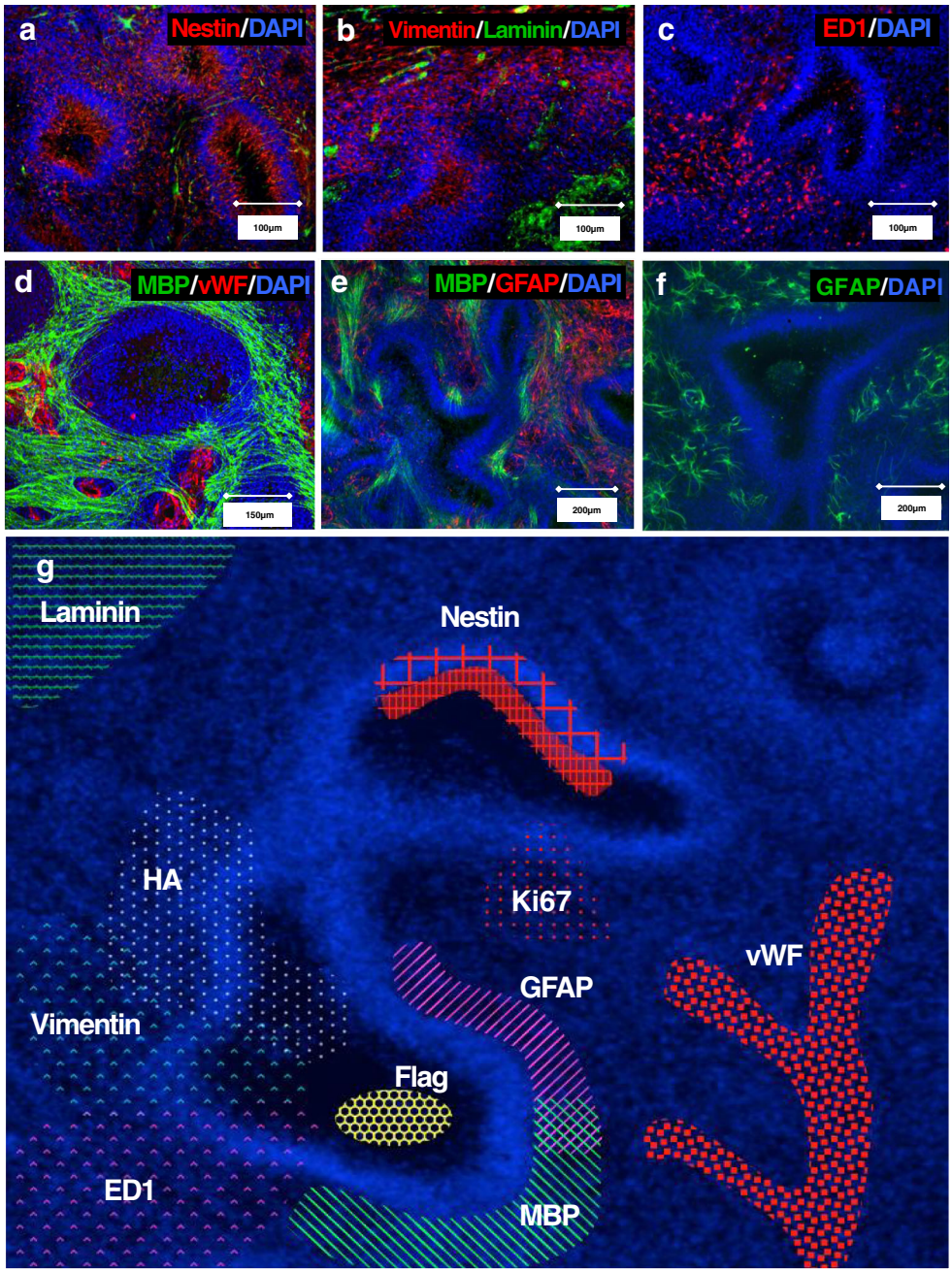

Fig. 3 The cellular composition of pseudopalisades. (A–C) Fluorescence confocal microscopy of pseudopalisades within high-grade *HRAS–G12V/PDGFB/AKT*-induced gliomas. The interior of pseudopalisades contain Nestin-positive (A) and Vimentin-positive (B) tumor cells. (C) ED1-positive microglia, (D) myelin basic protein (MBP)-positive myelinated neuronal axons, Von Willebrand factor (VWF)-positive (vWF^{+}) blood vessels, and (E, F) glial fibrillary acidic protein (GFAP)-positive reactive astrocytes are predominantly found outside of pseudopalisades. (G) Schematic summarizing the representative data from panels (A–F). The localization of various cell types are highlighted. DAPI = 4',6-diamidino-2-phenylindole; HA =human influenza hemagglutinin (used as a tag, marker)

contributions of oncogenes that mimic the oncogenic pathway activation in human malignant gliomas. In our model, within the RTK/RAS/PI(3)K pathway, HRAS–G12V gave the highest penetrance of glial tumors; PDGFB had low penetrance, but increased penetrance and tumor grade in combination with other oncogenes; and AKT had little-to-no impact on tumor progression or penetrance. Using this model system, we failed to detect an effect of *IDH1–R132H* point mutation on glioma penetrance or tumor progression. The predictable tumor growth afforded by the combination of *HRAS–G12V/PDGFB* allowed us to assess an experimental antiglioma therapy against malignant gliomas during early and late stages of growth. This model will serve as a robust platform to begin assessment of the efficacies of other novel antiglioma therapeutics.

Previous animal models (Table 2) have been built on manipulations of the *RTK/PI3K/HRAS-G12V* (i.e., proliferative) signaling pathway in order to reliably create tumors in mice and rats [17–19, 23–28]. In previous animal models, while deletion of *PTEN* is clearly an important driver, addition of oncogenic *AKT* and *RAS* are frequently required in combination with each other or with alterations *p53* or *RB* signaling for tumor formation. In our model, in the presence of wildtype *p53*, *RAS* was sufficient to generate highly penetrant gliomas.

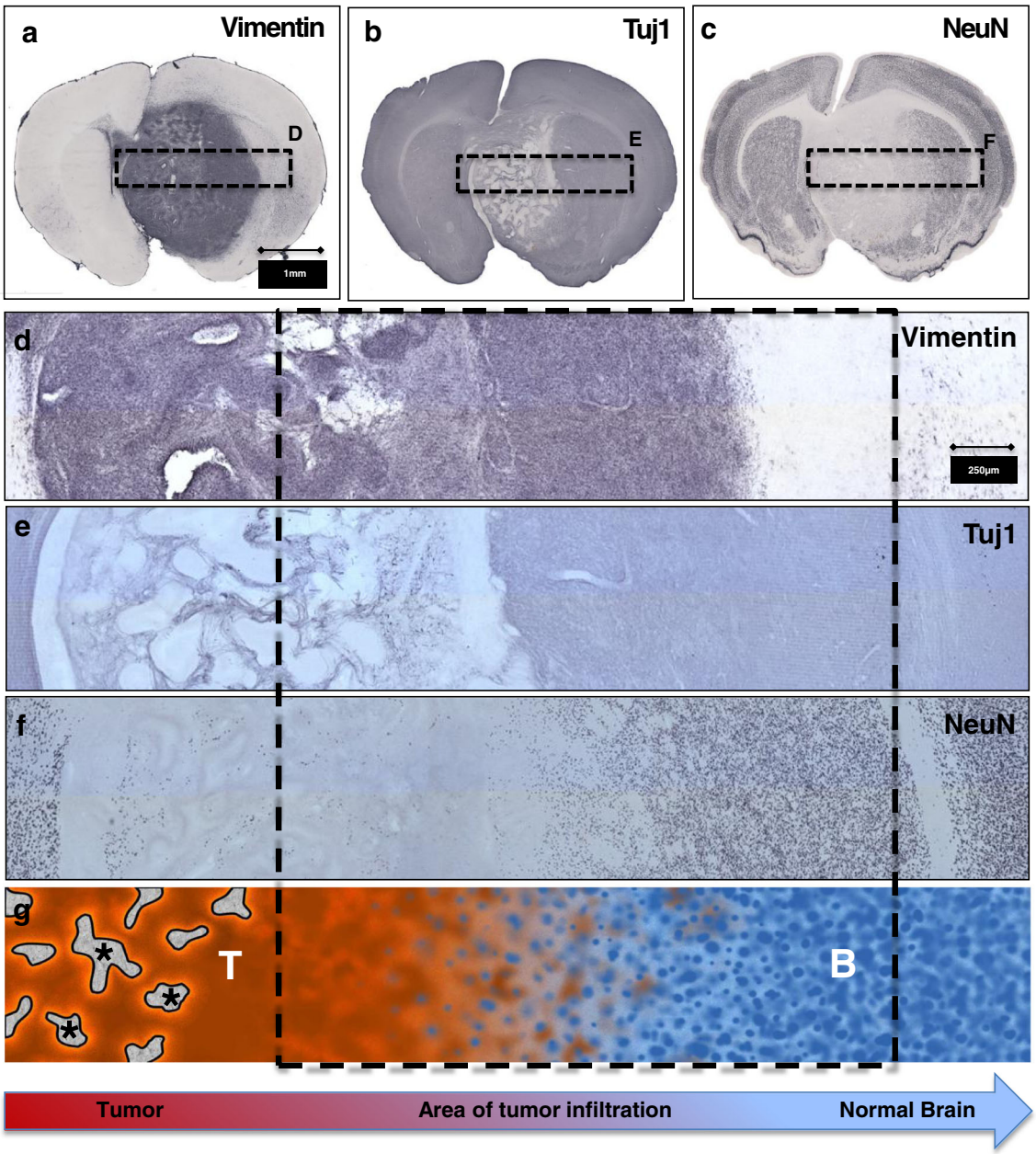

Fig. 4 Diffuse tissue infiltration of high-grade *de novo* gliomas. (A–C) Adjacent 60-mm-thick coronal tissue sections from a rat brain bearing a high-grade glioma induced by *HRAS–G12V*, *PDGFB*, and *AKT* stained with (A) Vimentin (tumor cells), (B) Tuj1 (neuronal axons), and (C) neuronal nuclei (NeuN). (D–G) High magnification images of the areas outlined by the black dotted boxes in (A–C), respectively. As illustrated by these higher magnification images, there are significant numbers of normal neurons trapped within the tumor tissue. (D–F) The infiltration of Vimentin-positive tumor cells into healthy tissue is visible when slides are aligned. (G) The schematic illustrates infiltrative tumor tissue into the surrounding normal brain. *Pseudopalisades within the tumor . T = tumor; B = normal brain

Within this pathway, *PDGF-B ligand* plays an important role, and is sufficient to form high-grade gliomas, albeit with a wide range of penetrance and clinical course when used individually [17, 18, 23]. Our results indicate that while *PDGFB* alone is sufficient to create high-grade gliomas, tumor penetrance is low. The combination of *PDGFB* with lentiviruses expressing HRAS–G12V increased tumor penetrance, hastened tumor progression, and induced uniformly malignant high-grade gliomas. Of all oncogenes tested, *HRAS–G12V* was the most consistent in driving gliomagenesis, although tumor progression was substantially protracted compared with gliomas induced with the combination of *HRAS–G12V* and *PDGFB*. Our work demonstrates that gliomagenesis in rats is dependent on the activation of signaling pathways stimulated by *HRAS–G12V* and *PDGFB*. Conversely, AKT had far less of an effect on tumor development and progression than has been described previously [19, 26]. In the study by Marumoto et al. [19], the combination of

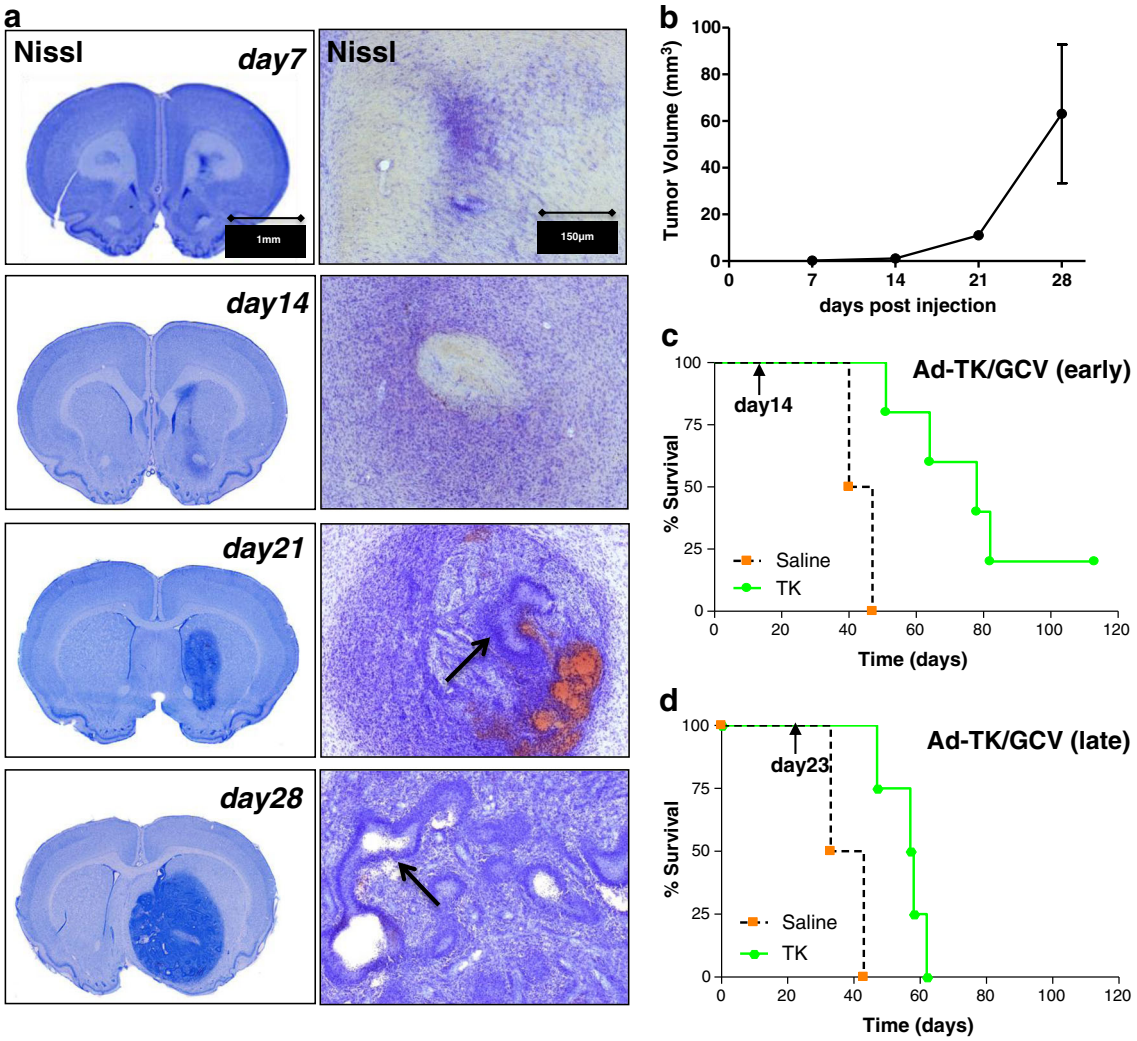

Fig. 5 Extent of tumor burden determines treatment efficacy of gene therapy against *de novo* gliomas. (A) Nissl staining of high-grade *de novo* gliomas induced by *HRAS–G12V/PDGFB/AKT* over time at low- (left) and high- (right) magnification. Tumor masses become visible 7 days post-lentiviral injection and grow progressively. By 21 days post-lentiviral injection, pseudopalisade-like structures (black arrows) can be identified. At 28 days post-lentiviral injection, there is extensive pseudopalisade formation in large tumors that comprise most of the striatum. (B) *HRAS–G12V/PDGFB/AKT* gliomas exhibit rapid growth, demonstrating the lack of impedance to tumor expansion. (C, D) *HRAS–G12V/PDGFB/AKT*-induced high-grade gliomas are sensitive to adenovirally mediated, conditionally cytotoxic gene therapy [adenovirus (serotype-5) expressing herpex simplex virus type 1-thymidine kinase (Ad-TK) plus systemically administered ganciclovir (GCV)] when treatment is initiated by day 14 post-lentiviral injection; (C) median survival increased by 25 %. However, gene therapy is less effective when initiated at (D) 23 days post-lentiviral injection, corresponding to greater tumor burden

lentiviral HRAS–G12V with AKT was required to produce highly penetrant gliomas in mice [19]. Possible reasons for this discrepancy are either species differences (highly penetrant gliomas were induced in wildtype *P53* rats), location of viral injections [subventricular zone and hippocampus in mice [19] *vs* striatum in rats (this study)], or cell of origin of glioma. In rats, low-volume injections were carefully placed in the striatum, reducing any chances of diffusion to the subventricular zone or hippocampus.

The choice of rodent species determines significant differences in the capacity to develop high-grade gliomas of high penetrance and short latency. In order to reach these practical goals for *de novo* glioma modeling in mice, genetic alterations decreasing the efficacy of the *TP53* and *RB* tumor suppressor genes have been necessary [16, 17, 23, 25, 27, 28]. In rats, our data confirm the results of Assanah et al. [18], suggesting that the need for *p53* inactivation in glioma may be species-dependent, and that the manipulation of the RTK/RAS/PI(3)K signaling pathway is sufficient to create gliomas in rats. There is evidence that neurogenesis in rats is higher than in mice, which might explain the increased tumorigenic response to manipulations of oncogenes in the proliferation pathways [29].

Human gliomas are genetically heterogeneous, and whether all mutations are required to be present in the same tumor cell or not remains to be determined. If we assume that noncell

Table 2 Summary of endogenous animal models of *de novo* gliomas

Author [Ref.]	Animal	System	Age/injection site	Proliferation (RTK/RAS/PI3K)	p53	Cell Cycle (Rb/INK4)	Penetrance (survival) Impact
Holland et. al, 2000 [26]	Mice	RCAS	Neonatal/frontal lobe	AKT, K-RAS	Wildtype	Wildtype	Combination AKT and K-RAS increases 27 % (0–27 %) compared with each alone
Dai et al., 2001 [23]	Mice	RCAS	Neonatal/frontal lobe	PDGF	$p53^{-/-}$ or $p53^{+/+}$	$INK4a^{-/-}$ or $INK4a^{+/+}$	INK4a loss increases 31 % (39–70 %), p53 loss has no impact (39–15 %)
Uhrbom et al., 2002 [28]	Mice	RCAS	NA	AKT, K-RAS	$ARF^{-/-}$	$INK4a^{-/-}$	INK4a loss increases 27 % in Ntv-a (21–48 %); 42 % in Gtv-a (0–42 %)
Dai et al., 2005 [24]	Mice	RCAS	NA	PDGF, K-RAS, AKT	Wildtype	Wildtype	Did not provide penetrance information
Hambardzumyan et al., 2009 [17]	Mice	RCAS	4.0–6.5 weeks	PDGF	$p53^{-/-}$ or $ARF^{-/-}$	$INK4a^{-/-}$ or $INK4a^{+/+}$	PDGF increases from 16 % (Ntv-A) and 22 % (Gtv-A) to 100 % (with INK4a loss or p53 loss)
Lei et al., 2011 [27]	Mice	Retrovirus	Adults/white matter	PDGF, $PTEN^{-/-}$ or $PTEN^{+/+}$	$p53^{-/-}$ or $p53^{+/+}$	Wildtype	PTEN loss increases 90 % (10–100 %)
Weisner et al., 2009 [16]	Mice	Sleeping beauty	Neonatal/R lateral ventricle	NRAS, AKT, SV40-LgT, EGFR	shp53 (plasmid)	Wildtype	Combination p53 and NRAS increases 60 % (0 %->60 %) combination AKT and NRAS increases 50 % (0 %->50 %)
Marumoto et al., 2009 [19]	Mice	Lentivirus	8–16 weeks/hippocampus/ SVZ	H-RAS, AKT	$p53^{-/-}$ or $p53^{+/+}$	Wildtype	p53 loss increases 59 % (41– 100 %)
de Vries et al., 2010 [25]	Mice	Lentivirus	8–16 weeks/cortex	K-RAS, $PTEN^{-/-}$ or $PTEN^{+/+}$	$p53^{+/+}$ or $p53^{-/-}$ $ARF^{-/-}$	$INK4a^{-/-}$	INK4a loss and K-RAS give 100 % (± PTEN or p53 loss); CMV promoter increases 50 % (50 % GFAP-Cre, 100 % CMV-Cre)
Assanah et al., 2006 [18]	Rats	Retrovirus	Adults/corpus collosum	PDGF	Wildtype	Wildtype	PDGF increases 100 % (vector 0 %)
Lynes et al.[this study]	Rats	Lentivirus	7–10 weeks/striatum	PDGF, H-RAS, AKT	Wildtype	Wildtype	HRAS 75 % alone, PDGF increases 25 % (75–100 %); IDH1-R132H and AKT has no impact

NA = not applicable; SVZ = subventricular zone; PDGF = platelet-derived growth factor; PTEN = phosphatase and tensin homolog; NRAS = neuroblastoma –RAS GTPose; EGFR = epidermal growth factor receptor; ARF = alternate reading frame of the CDKN2A locus; INK4a = inhibiting cyclin dependent kinase 4; CMV = cytomegalovirus; GFAP = glial fibrillary acidic protein; Rb = retinoblastoma protein; KRAS = Kirsten rat sarcoma GTPase; HRAS = Harvey rat sarcoma GTPase; AKT = "Ak strain" thymoma serine/theronine-specific protein kinase; RCAS-Ntv-A = Replication-competent ALV (avian leucosis virus) splice acceptor vector-nestin tumor virus A; RCAS-Gtv-A = Replication-competent ALV (avian leucosis virus) splice acceptor vector-glial fibrillary acidic protein tumor virus A

autonomous mutations must coexist in the same cell, one would need to show such coexistence at the time of infection and during tumor development. Owing to technical limitations we were unable to determine if individual cells were, indeed, coinfected in our tumors. Nevertheless, as *PDGFB* is secreted, its cooperativity with other cell-autonomous oncogenes is less dependent on coexpression in the same glioma cells.

We tested whether expression of glioma-associated *IDH1–R132H* contributes to tumor formation in rats. We failed to detect an effect of *IDH1–R132H* point mutation on glioma penetrance or tumor progression in our model. A potential limitation of our interpretation is that even though we showed biological effects of *IDH1–R132H* on histone methylation *in vitro* (suggested to contribute to oncogenesis in human glioblastoma [30]), we have yet to confirm similar biological effects in the gliomas in rats. The absence of effects of *IDH1–R132H* in our experiments could, potentially, be explained by functional differences in the activity of *IDH1* in rodents and humans [31]. Alternatively, recent clinical trial data in human patients show that *IDH1–R132H*, in addition to previously identified 1p19q loss of heterozygosity, substantially increases the response of adult glioma to treatment [32, 33]. If the main role of *IDH1–R132H* is to increase sensitivity to treatments, we would not predict seeing a direct influence on glioma formation in our untreated rodents. Regardless, further studies of the biological function of the IDH1–R132H mutation in animal models of glioma are warranted to help elucidate its contribution to gliomagenesis.

For models to be relevant for human GBM they need to replicate both the genetic changes and the histopathology of the human disease. Though not required for a pathological diagnosis, pseudopalisades are highly specific to glioblastoma, and consist of a hypercellular ring surrounding a predominantly necrotic core [34]. Previous papers have suggested that pseudopalisades are a highly mobile population of cells fleeing an area of hypoxia caused by thrombosed vessels [34]. Using our *HRAS–G12V*/*PDGFB*/*AKT* model, we performed a detailed investigation of pseudopalisade formation and the infiltrative capacity of high-grade gliomas. Contrary to previous observations, we failed to detect thrombosed vessels within the core of pseudopalisades. Notably, few neurons remain in the tumor area rich in pseudopalisades. This may indicate that pseudopalisades form late during tumor growth, once normal brain tissue has been effaced.

Treatment of *HRAS–G12V*/*PDGFB*/*AKT* tumors with the combination of Ad-TK and systemic ganciclovir was effective if administered at early time points, corresponding to low tumor burden. However, if tumors were left untreated until tumor burden was large, the therapy failed. This experiment demonstrates the utility of our endogenous glioma model as a platform for the testing of preclinical therapeutics.

Our work provides insight into the biogenesis and maturation of pseudopalisades, the identification of substantial invasion of normal brain tissue, and the contribution of individual genes to the formation of high- and low-grade gliomas. Furthermore, we demonstrate that this model can be used to test the pathogenic role of further mutations, such as those described in *IDH1*. With the availability of accurate, consistent, and robust preclinical animal models with high penetrance and predictable course of tumor progression, we will be able to test novel therapeutic approaches to combat this lethal disease.

Acknowledgments This work was supported by National Institutes of Health/National Institute of Neurological Disorders & Stroke (NIH/NINDS) grants 1RO1-NS 054193, 1RO1-NS 061107, and 1RO1-NS082311 to P.R.L.; and grants 1UO1-NS052465, 1RO1-NS 057711, and 1RO1-NS074387 to M.G.C. We thank Drs. I. Verma, E.C. Holland, and P. Canoll for providing valuable expression vectors utilized in this work. We thank Mr. Philip Jenkins and the Department of Neurosurgery at the University of Michigan, School of Medicine for their support of our work. We also thank Dr. Karin Murasko for her academic leadership, and D. Tomford and S. Napolitan for superb administrative support. The schematic of tumor infiltration (Fig. 4G) was created by Alan Traxler (alan.traxler@gmail.com). Full conflict of interest disclosure is available in the electronic supplementary material for this article.

Required Author Forms Disclosure forms provided by the authors are available with the online version of this article.

References

1. Louis DN, Ohgaki H, Wiestler OD, et al. The 2007 WHO classification of tumours of the central nervous system. Acta Neuropathol 2007;114:97-109.
2. Grossman SA, Ye X, Piantadosi S, et al. Survival of patients with newly diagnosed glioblastoma treated with radiation and temozolomide in research studies in the United States. Clin Cancer Res 2010;16:2443-2449.
3. Kruse CA, Molleston MC, Parks EP, et al. A rat glioma model, CNS-1, with invasive characteristics similar to those of human gliomas: a comparison to 9L gliosarcoma. J Neurooncol 1994;22:191-200.
4. Barker M, Hoshino T, Gurcay O, et al. Development of an animal brain tumor model and its response to therapy with 1,3-bis(2-chloroethyl)-1-nitrosourea. Cancer Res 1973;33:976-986.
5. Aas AT, Brun A, Blennow C, et al. The RG2 rat glioma model. J Neurooncol 1995;23:175-183.
6. Benda P, Lightbody J, Sato G, et al. Differentiated rat glial cell strain in tissue culture. Science 1968;161:370-371.
7. Chen J, McKay RM, Parada LF. Malignant glioma: lessons from genomics, mouse models, and stem cells. Cell 2012;149:36-47.
8. Hambardzumyan D, Parada LF, Holland EC, et al. Genetic modeling of gliomas in mice: new tools to tackle old problems. Glia 2011;59:1155-1168.
9. Chow LM, Baker SJ. Capturing the molecular and biological diversity of high-grade astrocytoma in genetically engineered mouse models. Oncotarget 2012;3:67-77.
10. Dunn GP, Rinne ML, Wykosky J, et al. Emerging insights into the molecular and cellular basis of glioblastoma. Genes Dev 2012;26:756-784.
11. Cancer Genome Atlas Research Network. Comprehensive genomic characterization defines human glioblastoma genes and core pathways. Nature 2008;455:1061-1068.

12. Parsons DW, Jones S, Zhang X, et al. An integrated genomic analysis of human glioblastoma multiforme. Science 2008;321: 1807-1812.
13. Turcan S, Rohle D, Goenka A, et al. IDH1 mutation is sufficient to establish the glioma hypermethylator phenotype. Nature 2012;483: 479-483.
14. Ducray F, Marie Y, Sanson M. IDH1 and IDH2 mutations in gliomas. N Engl J Med 2009;360:2248-2249.
15. Bonavia R, Inda MM, Cavenee WK, et al. Heterogeneity maintenance in glioblastoma: a social network. Cancer Res 2011;71: 4055-4060.
16. Wiesner SM, Decker SA, Larson JD, et al. De novo induction of genetically engineered brain tumors in mice using plasmid DNA. Cancer Res 2009;69:431-439.
17. Hambardzumyan D, Amankulor NM, Helmy KY, et al. Modeling Adult Gliomas Using RCAS/t-va Technology. Transl Oncol 2009;2: 89-95.
18. Assanah M, Lochhead R, Ogden A, et al. Glial progenitors in adult white matter are driven to form malignant gliomas by platelet-derived growth factor-expressing retroviruses. J Neurosci 2006;26:6781-6790.
19. Marumoto T, Tashiro A, Friedmann-Morvinski D, et al. Development of a novel mouse glioma model using lentiviral vectors. Nat Med 2009;15:110-116.
20. Dewey RA, Morrissey G, Cowsill CM, et al. Chronic brain inflammation and persistent herpes simplex virus 1 thymidine kinase expression in survivors of syngeneic glioma treated by adenovirus-mediated gene therapy: implications for clinical trials. Nat Med 1999;5:1256-1263.
21. Capper D, Weissert S, Balss J, et al. Characterization of R132H mutation-specific IDH1 antibody binding in brain tumors. Brain Pathol 2010;20:245-254.
22. Puntel M, Kroeger KM, Sanderson NS, et al. Gene transfer into rat brain using adenoviral vectors. Curr Protoc Neurosci 2010;Chapter 4: Unit 4.24.
23. Dai C, Celestino JC, Okada Y, et al. PDGF autocrine stimulation dedifferentiates cultured astrocytes and induces oligodendrogliomas and oligoastrocytomas from neural progenitors and astrocytes in vivo. Genes Dev 2001;15:1913-1925.
24. Dai C, Lyustikman Y, Shih A, et al. The characteristics of astrocytomas and oligodendrogliomas are caused by two distinct and interchangeable signaling formats. Neoplasia 2005;7:397-406.
25. de Vries NA, Bruggeman SW, Hulsman D, et al. Rapid and robust transgenic highgrade glioma mouse models for therapy intervention studies. Clin Cancer Res 2010;16:3431-3441.
26. Holland EC, Celestino J, Dai C, et al. Combined activation of Ras and Akt in neural progenitors induces glioblastoma formation in mice. Nat Genet 2000;25:55-57.
27. Lei L, Sonabend AM, Guarnieri P, et al. Glioblastoma models reveal the connection between adult glial progenitors and the proneural phenotype. PLoS One 2011;6:e20041.
28. Uhrbom L, Dai C, Celestino JC, et al. Ink4a-Arf loss cooperates with KRas activation in astrocytes and neural progenitors to generate glioblastomas of various morphologies depending on activated Akt. Cancer Res 2002;62:5551-5558.
29. Snyder JS, Choe JS, Clifford MA, et al. Adult-born hippocampal neurons are more numerous, faster maturing, and more involved in behavior in rats than in mice. J Neurosci 2009;29:14484-14495.
30. Lu C, Ward PS, Kapoor GS, et al. IDH mutation impairs histone demethylation and results in a block to cell differentiation. Nature 2012;483:474-478.
31. Atai NA, Renkema-Mills NA, Bosman J, et al. Differential activity of NADPHproducing dehydrogenases renders rodents unsuitable models to study IDH1R132 mutation effects in human glioblastoma. J Histochem Cytochem 2011;59:489-503.
32. Shaw EG, Wang M, Coons SW, et al. Randomized trial of radiation therapy plus procarbazine, lomustine, and vincristine chemotherapy for supratentorial adult low-grade glioma: initial results of RTOG 9802. J Clin Oncol 2012;30:3065-3070.
33. Erdem-Eraslan L, Gravendeel LA, de Rooi J, et al. Intrinsic molecular subtypes of glioma are prognostic and predict benefit from adjuvant procarbazine, lomustine, and vincristine chemotherapy in combination with other prognostic factors in anaplastic oligodendroglial brain tumors: a report from EORTC study 26951. J Clin Oncol 2013;31:328-336.
34. Brat DJ, Castellano-Sanchez AA, Hunter SB, et al. Pseudopalisades in glioblastoma are hypoxic, express extracellular matrix proteases, and are formed by an actively migrating cell population. Cancer Res 2004;64:920-927.